

SUPPLEMENTARY INFORMATION

Organization of the inputs and outputs of the mouse superior colliculus

Nora L. Benavidez¹⁻³, Michael S. Bienkowski², Muye Zhu^{2,3}, Luis H. Garcia^{2,3}, Marina Fayzullina^{2,3}, Lei Gao^{2,3}, Ian Bowman^{2,3}, Lin Gou^{2,3}, Neda Khanjani², Kaelan R. Cotter^{2,3}, Laura Korobkova^{1,2}, Marlene Becerra², Chunru Cao^{2,3}, Monica Y. Song¹⁻³, Bin Zhang^{2,3}, Seita Yamashita^{2,3}, Amanda J. Tugangui^{2,3}, Brian Zingg^{2,3}, Kasey Rose¹, Darrick Lo^{2,3}, Nicholas N. Foster^{2,3}, Sarvia Aquino², Tyler Boesen^{2,3}, Hyun-Seung Mun^{2,3}, Ian R. Wickersham⁴, Giorgio A. Ascoli⁵, Houri Hintiryan^{2,3} & Hong-Wei Dong^{2,3*}

¹ Neuroscience Graduate Program, University of Southern California, Los Angeles, CA 90033, USA.

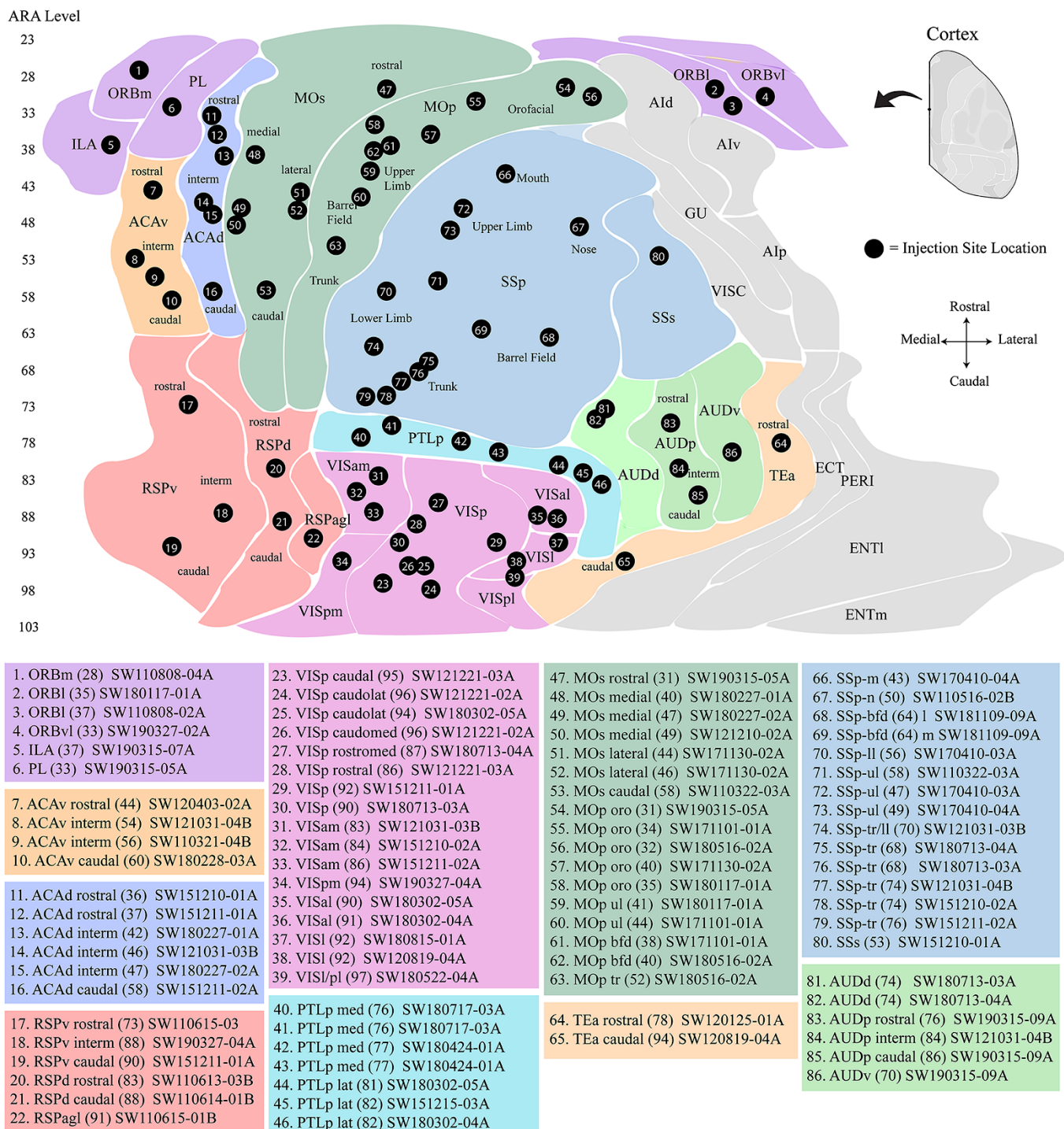
² Stevens Neuroimaging and Informatics Institute, Laboratory of Neuro Imaging, Keck School of Medicine, University of Southern California, Los Angeles, CA 90033, USA.

³ Current affiliation: UCLA Brain Research & Artificial Intelligence Nexus, Department of Neurobiology, David Geffen School of Medicine, University of California Los Angeles, Los Angeles, CA 90095, USA.

⁴ McGovern Institute for Brain Research, Massachusetts Institute of Technology, Cambridge, MA 02139, USA.

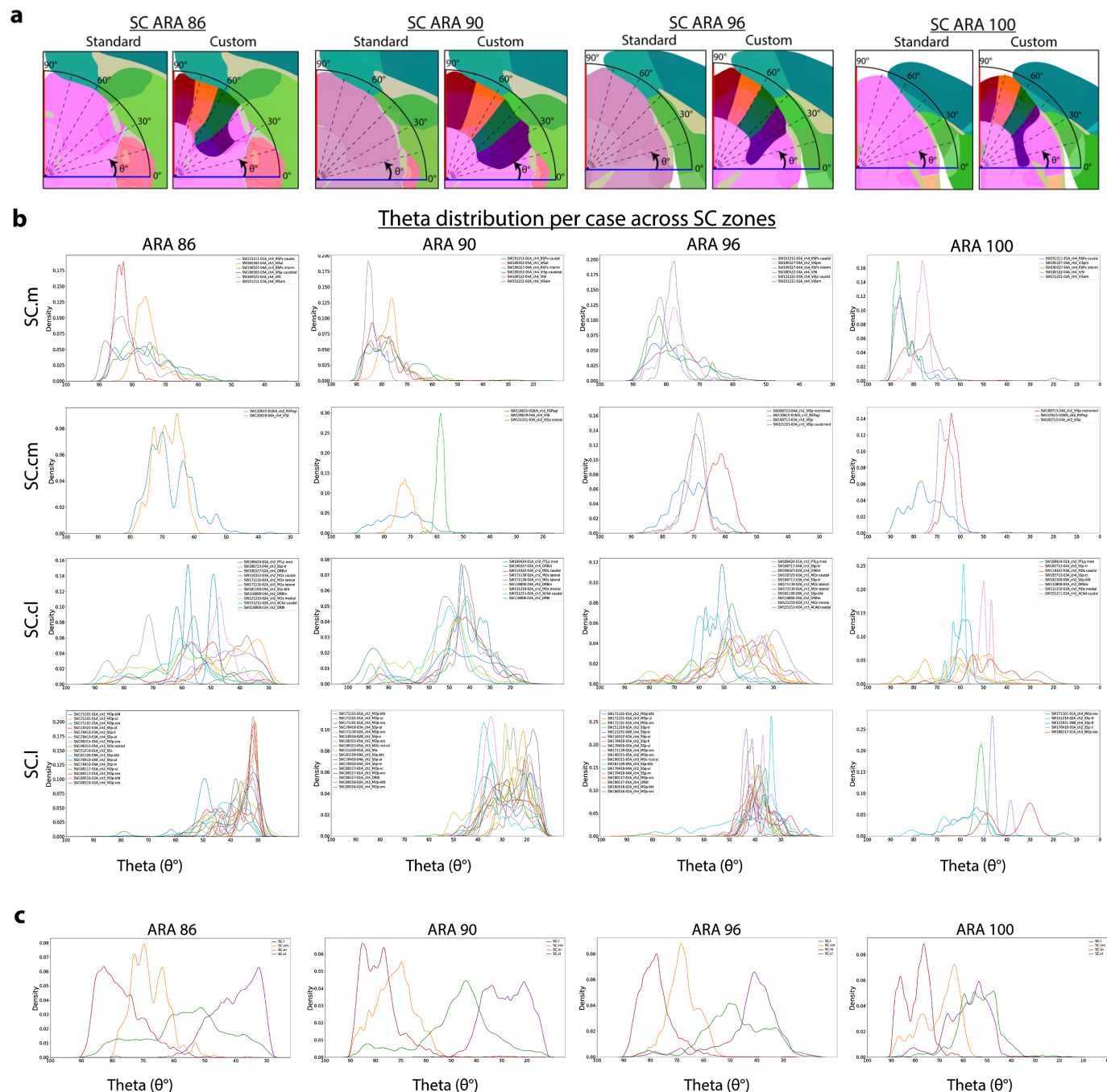
⁵ Krasnow Institute for Advanced Study, George Mason University, Fairfax, VA 22030, USA.

*Corresponding author: Hong-Wei Dong, M.D., Ph.D. (hongweid@mednet.ucla.edu)



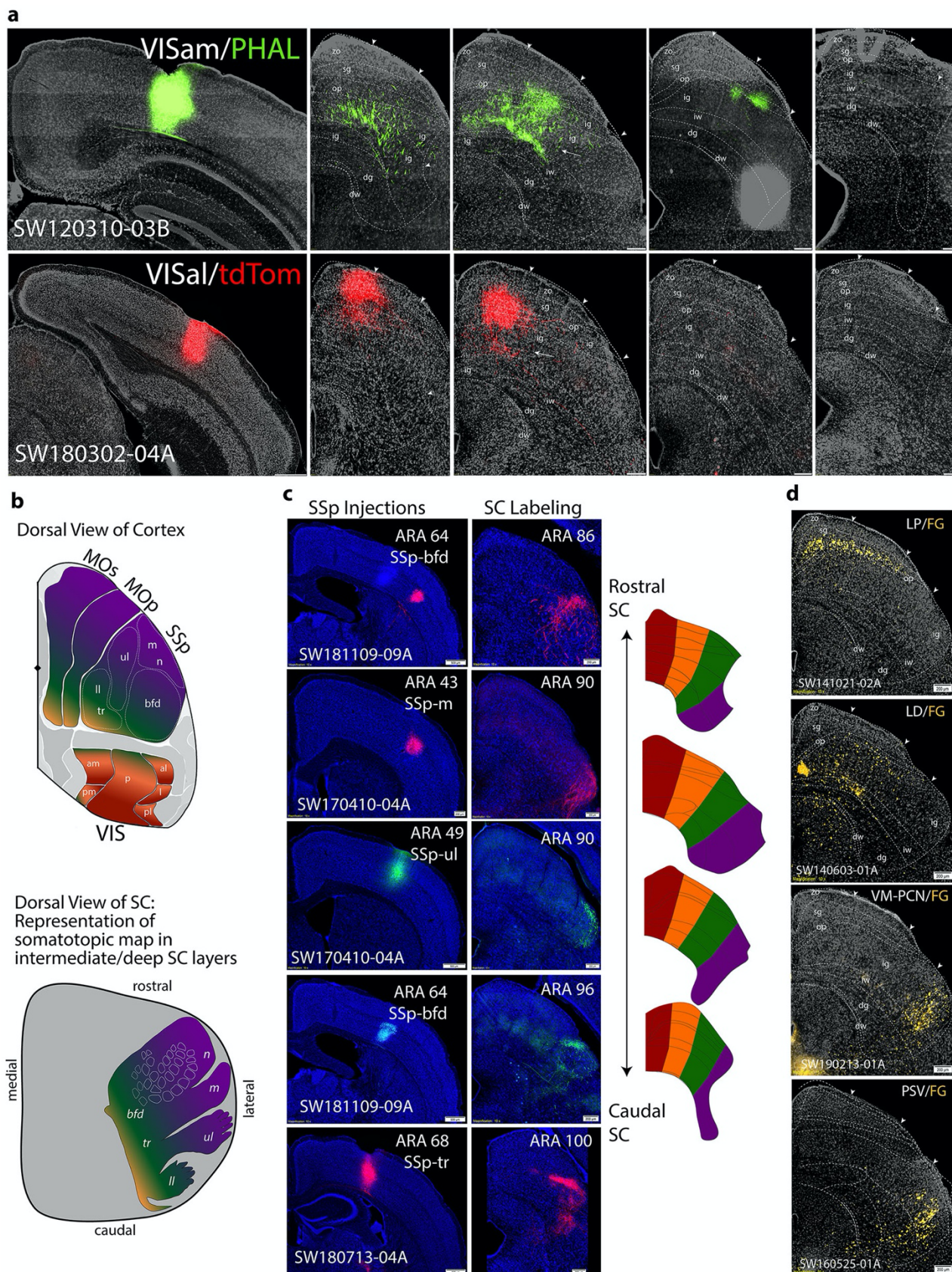
Supplementary Figure 1 | Flat map of mouse cortex with injection sites names.

Shaded brain region corresponds to same shaded color box with corresponding numbers for each case. Generated by expanding the length of each cortical area from the coordinate framework on the Allen Institute Adult Mouse Brain Atlas. Filled circles indicate location of injection site. List of injection sites, coordinates, and location can be cross-referenced by index number with Supplementary Table 2.



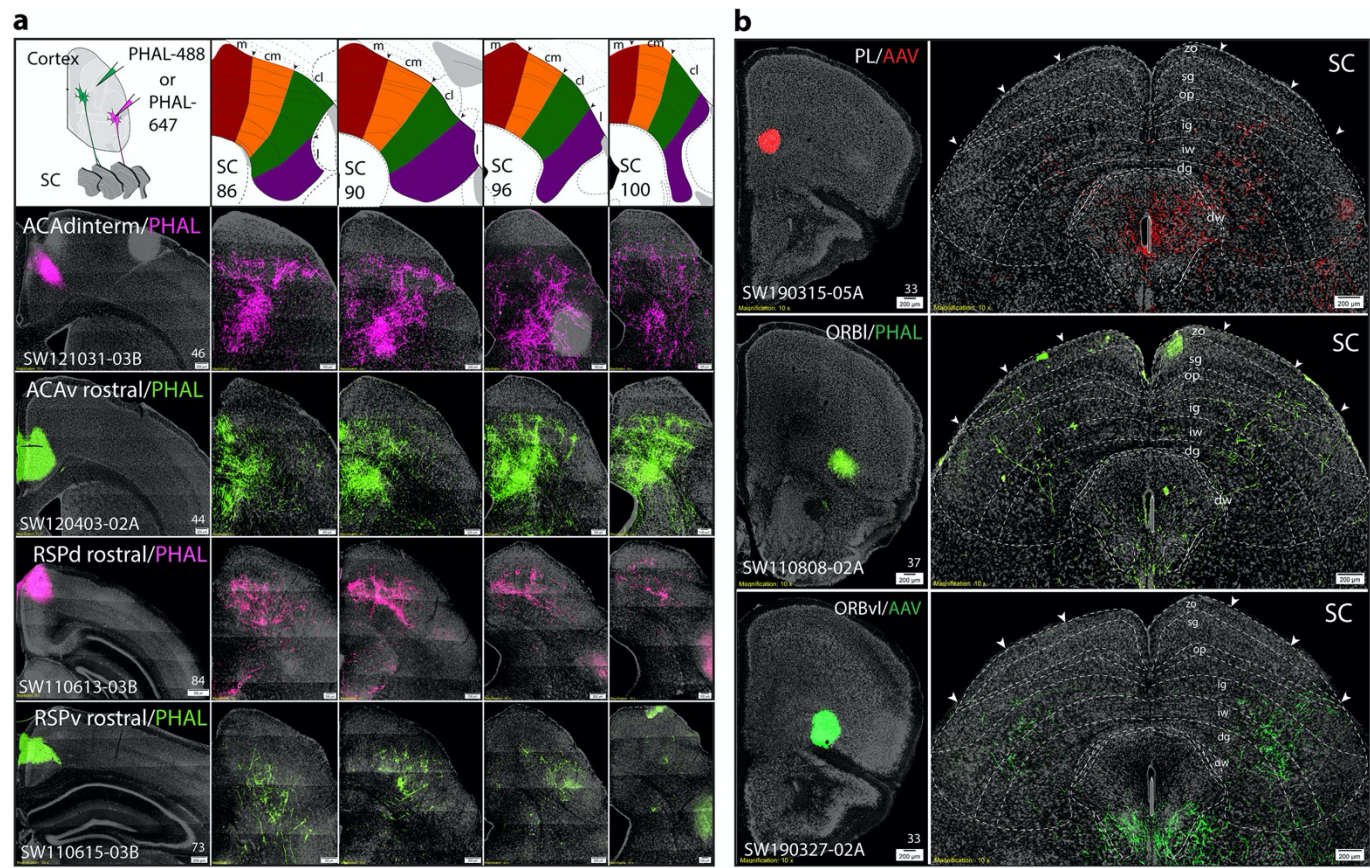
Supplementary Figure 2 | Probability distribution plots.

a) Atlas levels for the SC from rostral to caudal: ARA levels 86, 90, 96, and 100. Left side is polar coordinate ranges used to quantify angular distribution of thresholded pixel labeling in SC. Angles represented by theta (θ°) values where midline starts at 90° and ranges toward 0° at lateral angles. Right side is the custom SC atlas with overlay of angular range showing coarse alignment of manually delineated borders in SC. Color-code associations: red (SC.m), orange (SC.cm), green (SC.cl), purple (SC.l). **b)** Probability distribution plots organized by individual cortical cases that target distinct zones. SC.m, SC.cm, SC.cl, and SC.l. *X*-axis represents pixel density, *y*-axis represents theta angle from medial to lateral. Columns of panels are organized by ARA level displaying plots of individual cases that preferentially target to each SC zone. Top row plots from cases that target SC.m (n=7), next row SC.cm (n=4), next row SC.cl (n=12), and last row SC.l (n=20). **c)** Average of probability distribution plots from multiple cases. Average is based on cases from data in b.



Supplementary Figure 3 | Sensory related connectivity with SC.

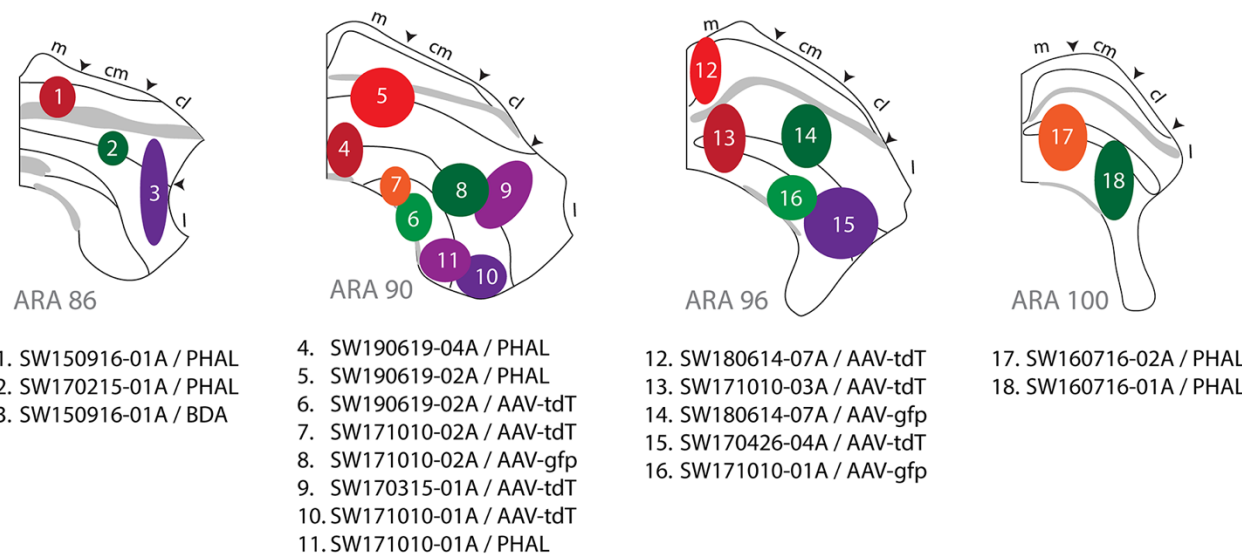
a) Raw data of higher order visual areas VISam and VISal. A PHAL injection into VISam (SW120310-03B) projects mainly to intermediate layers in SC.cm, with some terminals in superficial layers. An AAV-tdTomato injection into VISal (SW18080302-04A) projects densely to superficial layers of SC.m with some fibers in the intermediate layers. **b)** Within the cortex, somatic sensorimotor areas are each organized into distinct highly interconnected subnetworks that integrate the somatotopic body map and project subcortically to the SC. Body parts include mouth (m), nose (n), upper limb (ul), lower limb (ll), barrel-field (bfd), and trunk (tr). The dorsal view of the cortical map is color-coded with the dorsal view of the SC body part region it projects to (consistent with the color-coded zones in the SC custom atlas). This organization is conserved topographically as illustrated by dorsal view of SC with overlayed homunculus of somatosensory body representation. **c)** Injection sites into distinct SSp regions project to adjacent and distinct SC.l or SC.cl zones across rostral to caudal levels show adjacent body part projections. Color-code associations: red (SC.m), orange (SC.cm), green (SC.cl), purple (SC.l). Scale bars are 200 μ m for all SC panels; 500 μ m for injection site panels. **d)** Retrograde labeling of fluorogold (FG)-labeled cells in the SC from four separate injections. First panel: injection into the lateroposterior nucleus of thalamus (LP) back-labeled cells across superficial layers in SC.m and SC.cm zones. Second panel: injection into the laterodorsal nucleus of thalamus (LD) back-labeled cells across superficial and intermediate layers predominantly in SC.cm and SC.m, with sparse cells in SC.cl. Third panel: injection into the ventromedial nucleus (VM) and paracentral nucleus of thalamus (PCN) back-labeled cells in the intermediate and deep layers confined to the SC.l zone.



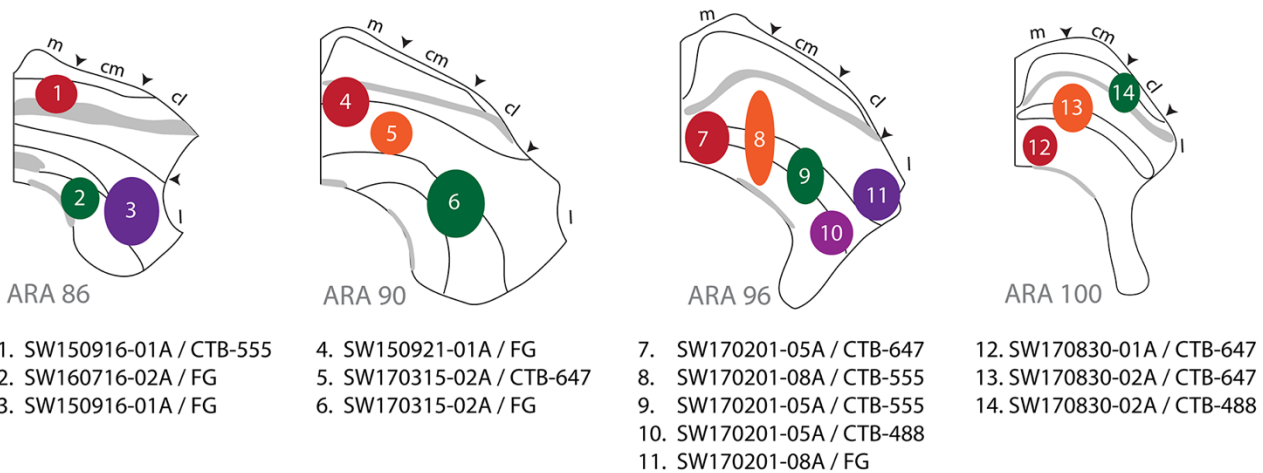
Supplementary Figure 4 | Higher-order cortico-tectal arrays.

a) Data array of individual cases from higher order projections to SC. Injection sites from top to bottom: ACAd-intermediate, ACAv-rostral, RSPd-rostral, RSPv-rostral. **b)** Three cases with single anterograde injections into PL (AAV), ORBI (PHAL), and ORBvl with their respective bilateral projections predominately to SC.cl and SC.l zones at ARA 90. Scale bars are 200 μm.

a Anterograde Injections in Superior Colliculus

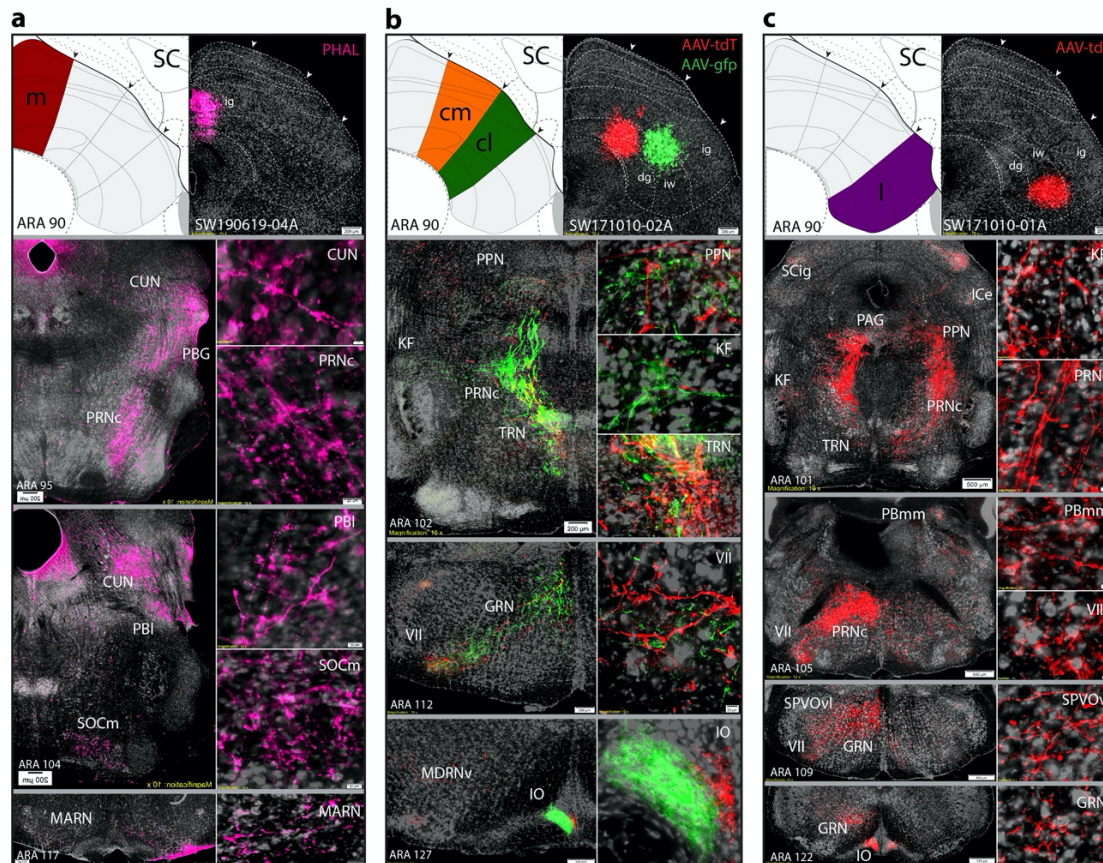


b Retrograde Injections in Superior Colliculus



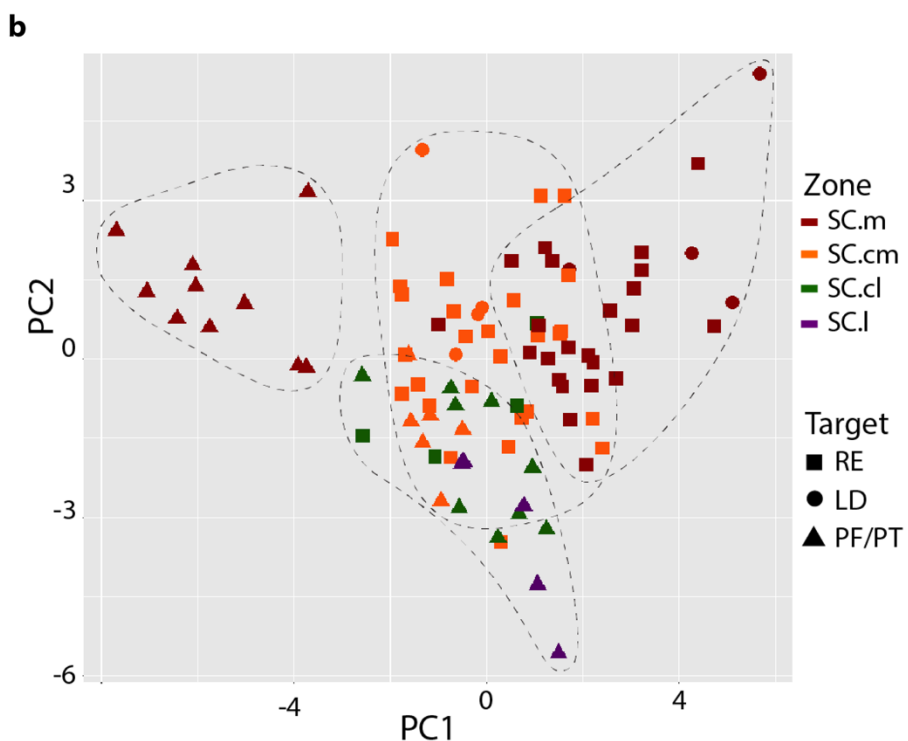
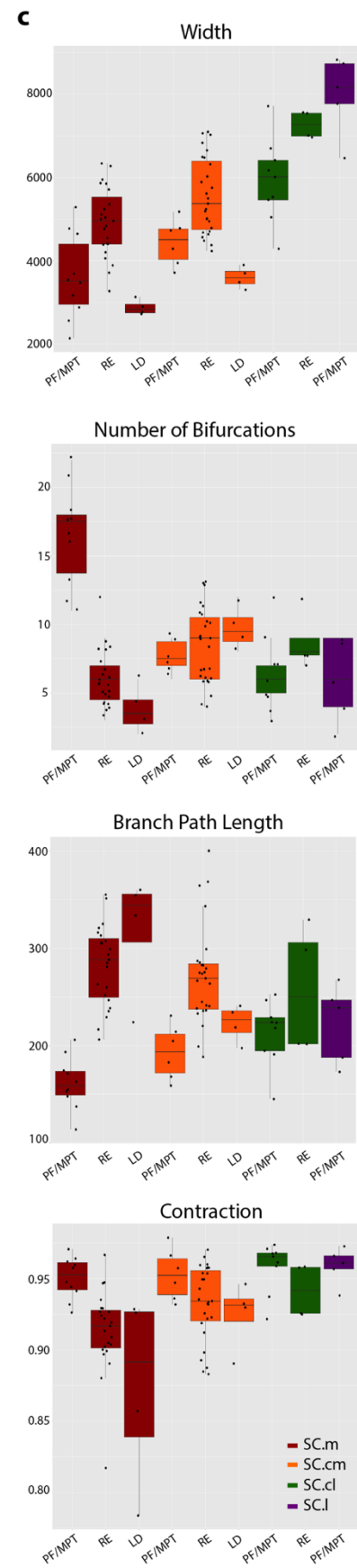
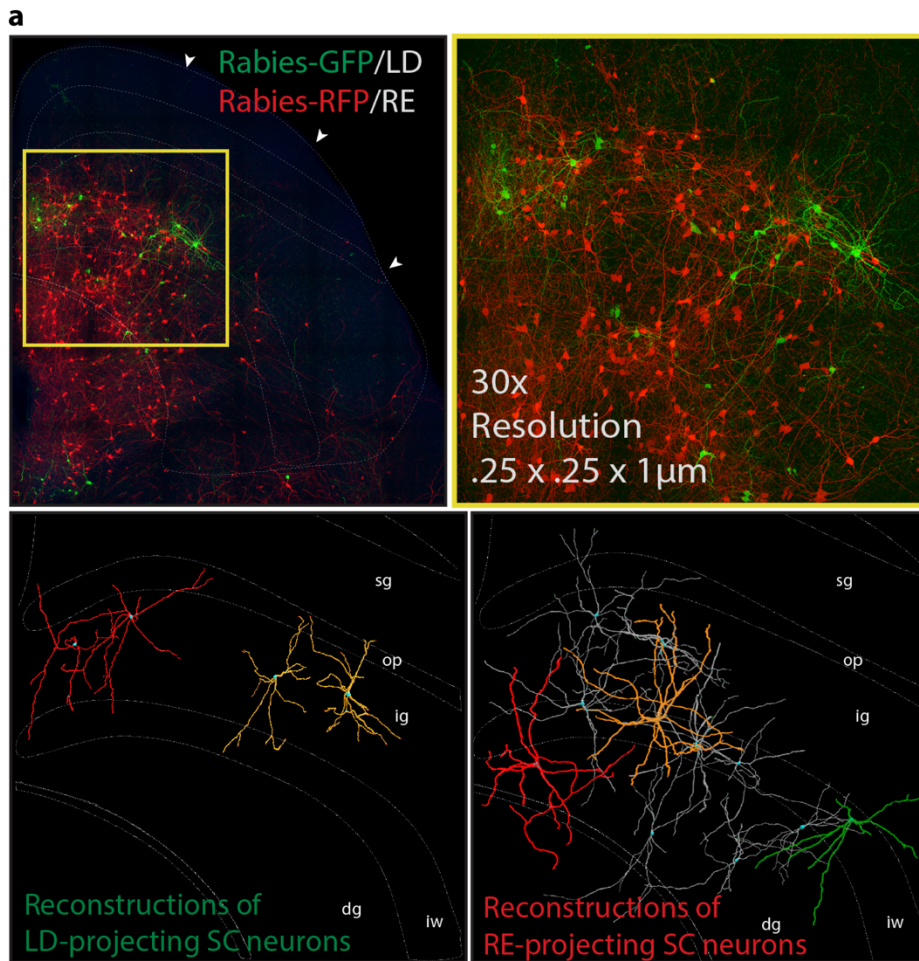
Supplementary Figure 5 | Injection sites in SC.

a) Anterograde injection sites in superior colliculus. **b)** Retrograde injection sites. The list can be cross-referenced with Supplementary Table 2 for complete details of injection sites, coordinates, and locations. Color-code associations: red (SC.m), orange (SC.cm), green (SC.cl), purple (SC.l). Abbreviations: AAV, adeno-associated virus; AAV-tdT, AAV-tdTomato; AAV-gfp, AAV-green fluorescent protein; ARA, Allen Reference Atlas; BDA, biotinylated dextran amine; CTB, cholera toxin subunit B conjugates (488, 555, 567); FG, Fluorogold; PHAL, phaseolus vulgaris leucoagglutinin; SC, superior colliculus; m, medial zone; cm, centromedial zone; cl, centrolateral zone; l, lateral zone.



Supplementary Figure 6 | Downstream projections from distinct SC zones to brainstem regions.

a) PHAL injection into SC.m-ig show prominent ipsilateral projections to midbrain and hindbrain regions. **b)** AAV-tdTomato injection into SC.cm-ig/iw and AAV-gfp injection into SC.cl-ig/iw produce downstream targets similar brainstem regions, with segregated but adjacent outputs in IO. **c)** Downstream projections from AAV-tdTomato injection in SC.l in intermediate white and deep grey layers. See Supplementary Table 1 for complete list of abbreviations. **d)** Quantification of four anterograde injections into each SC zone. Plots represent reconstructed pixel data from output projection terminals of SC throughout the brain. Distributions to contralateral and ipsilateral brain regions are shown, with brain regions organized based on ontological hierarchy in the Allen Reference Atlas (y-axis). Data normalization assigns values based on minimum threshold pixel value (0.0006) and maximum threshold pixel value (1) which represents the brain region that receives the highest value of pixels (x-axis).



Supplementary Figure 7 | Characterization of neuronal cell types in the SC based on their anatomical locations, projection targets and neuronal morphology.

a) LD projecting neurons in SC labeled with rabies-GFP in SC.m/cm-ig, and RE projecting neurons labeled with rabies-RFP injected into cells in SC.m/cm-ig/iw/dg. Tissue was processed by the SHIELD clearing protocol and followed by confocal imaging for 3D-reconstruction. Dendrites from LD and RE-projecting SC neurons were reconstructed to visualize differences and dendritic arborizations across SC layers and zones. The LD-projecting SC.m/SC.cm neurons had pyramidal-shaped cell bodies with dendrites that extended dorsally to the superficial optic layers and within the intermediate layers. Of the RE-projecting SC.m/cm neurons, some had dendrites that extended into superficial and intermediate layers, with others that extended into intermediate and deep layers. A subset of neurons extends dendrites horizontally, suggesting they integrate information within the same layer across zones. Other neurons extend vertically, suggesting these receive multimodal information integrated within multiple SC layers. **b)** Principal component analysis (PCA) shows segregation of zone- and target-specific cells based on measured morphological features (see Methods). Number of SC projection neuron reconstructions to RE (n=54), LD (n=8), and PF/MPT (n=31). **c)** Data are presented as whisker plots, where the center line represents the median, box limits show the upper and lower quartiles, and the whiskers represent the minimum and maximum data values. Examples of reports from pairwise tests of morphological parameters that survived the false discovery rate correction tests. Width measures the overall arbor size of neurons. RE-projecting cells in SC.cl and PF/MPT-projecting cells in SC.l are more than twice the width of LD-projecting cells in SC.m. Number of bifurcations compartmentalizes the arborizations into functionally distinct synaptic integration elements. Branch length represents a ratio between the width and number of bifurcations measures, and provides an indication of how they co-vary. It also relates to the number of synapses that can be received on a single computational element. Contraction measures the efficient occupancy of space to reach as many axonal boutons as possible in nearby and further distances. P-values for all parameters can be found in Supplementary Table 6. Abbreviations: LD, laterodorsal nucleus; PF/MPT, parafascicular nucleus of thalamus/midbrain pretectal area; RE, reuniens nucleus of thalamus; SC, superior colliculus; SC layers: zo, zonal; sg, superficial grey; op, optic; ig, intermediate grey; iw, intermediate white; dg, deep grey; dw, deep white.

Supplementary Table 1 | Brain Region Abbreviation List.

- ACAd**, Anterior cingulate area cortex, dorsal part
ACAv, Anterior cingulate area cortex, ventral part
AD, Anterodorsal nucleus thalamus
AId, Agranular insular area, dorsal part
AIv, Agranular insular area, ventral part
AIp, Agranular insular area, posterior part
APN, Anterior pretectal nucleus
AUDd, Auditory cortex, dorsal part
AUDp, Primary auditory cortex
AUDv, Auditory cortex, ventral part
AV, Anteroventral nucleus thalamus
BLA, Basolateral amygdalar nucleus
 BLAa, Basolateral amygdalar nucleus, anterior part
 BLAp, Basolateral amygdalar nucleus, posterior part
BMA, Basomedial amygdalar nucleus
 BMAa, Basomedial amygdalar nucleus, anterior part
 BMAP, Basomedial amygdalar nucleus, posterior part
CA1, Field CA1, hippocampal formation
CA3, Field CA3, hippocampal formation
CLA, Claustrum
CM, Centromedial nucleus thalamus
CP, Caudate putamen
 CPc.d, Caudate putamen, caudal, dorsal domain
 CPi.dl, Caudate putamen, intermediate, dorsolateral domain
 CPi.vl, Caudate putamen, intermediate, ventrolateral domain
 CPi.vm, Caudate putamen, intermediate, ventromedial domain
 CPr, Caudate putamen, rostral
CUN, Cuneate nucleus
DN, Dentate nucleus
DG, Dentate gyrus
DTN, Dorsal tegmental nucleus
ENT, Entorhinal cortex
GRN, Gigantocellular reticular nucleus,
GU, Gustatory cortex
Hb, Habenula nucleus thalamus
IAM, Interanteromedial nucleus thalamus
ICe, Inferior colliculus, external part
ILA, Infralimbic area cortex
IO, Inferior olfactory nucleus
IRN, Intermediate reticular nucleus
KF, Koelliker-Fuse subnucleus
LA, Lateral amygdalar area
LD, Laterodorsal nucleus thalamus
LG, Lateral geniculate nucleus thalamus
LP, Lateroposterior nucleus thalamus

LM, Lateral mammillary nucleus
MARN, Magnocellular reticular nucleus
MD, Mediodorsal nucleus thalamus
MDRNv, Medullary reticular nucleus, ventral part
MOp, Primary motor cortex
 MOp-oro, Primary motor cortex, orofacial part
MOs, Secondary motor cortex
MOs-fef, Secondary motor cortex, frontal eye field
MRN, Midbrain reticular nucleus
MPT, Midbrain pretectal region
ORBl, Orbitofrontal area cortex, lateral part
ORBm, Orbitofrontal area cortex, medial part
ORBvl, Orbitofrontal area cortex, ventrolateral part
PAG, Periaqueductal gray nucleus
 PAG.dl, Periaqueductal gray nucleus, dorsolateral part
 PAG.vl, Periaqueductal gray nucleus, ventrolateral part
PAR, Parasubiculum
PARN, Parvicellular reticular nucleus
PBG, Parabigeminal nucleus
PBI, Parabrachial nucleus, lateral part
PBmm, Parabrachial nucleus, mediomedial part
PCN, Pericentral nucleus thalamus
PERI, Perirhinal area cortex
PF, Parafascicular nucleus
 PF.II, Parafascicular nucleus, lower limb
 PF.m, Parafascicular nucleus, mouth domain
 PF.tr, Parafascicular nucleus, trunk domain
 PF.ul, Parafascicular nucleus, upper limb domain
PGRNI, Paragigantocellular reticular nucleus, lateral part
PL, Prelimbic area cortex
PP, Peripenduncular nucleus
PPN, Pedunculopontine nucleus
POST, Postsubiculum
PRE, Presubiculum
PRNc, Pontine reticular nucleus, caudal part
PSV, Principal sensory nucleus of the trigeminal
PTLp, Posterior parietal cortex
RE, Reuniens nucleus thalamus
RSPagl, Retrosplenial area cortex, agranular part
RSPd, Retrosplenial area cortex, dorsal part
RSPv, Retrosplenial area cortex, ventral part
SC, Superior colliculus
 SC.m, Superior colliculus, medial zone
 SC.cm, Superior colliculus, centromedial zone
 SC.cl, Superior colliculus, centrolateral zone
 SC.l, Superior colliculus, lateral zone
SI, Substantia innominata

SNc, Substantia nigra pars compacta

SNr, Substantia nigra pars reticulata

SOCm, Superior olfactory complex, medial part

SPFPp, Subparafascicular nucleus, parvicellular part

SPVOL, Spinal motor nucleus of trigeminal, oral lateral part

SPVOvl, Spinal motor nucleus of trigeminal, oral ventrolateral part

SSp, Somatosensory cortex primary

SSp-bfd, Somatosensory cortex primary, barrel field

SSp-ll, Somatosensory cortex primary, lower limb

SSp-m, Somatosensory cortex primary, mouth

SSp-n, Somatosensory cortex primary, nose

SSp-tr, Somatosensory cortex primary, trunk

SSp-ul, Somatosensory cortex primary, upperlimb

SSs, Somatosensory cortex, supplementary

STN, Subthalamic nucleus

SUB, Subiculum

SUBd, Subiculum dorsal

SUBdd, Subiculum dorsal, dorsal part

SUBdv, Subiculum dorsal, ventral part

ProSUB, Prosubiculum

SUBv, Subiculum ventral

SUBvv, Subiculum ventral, ventral tip

TEa, Temporal association area

TRN, Tegmental reticular nucleus

V, Trigeminal cranial nucleus

VII, Facial motor cranial nucleus

VISC, Visceral cortex

VISal, Visual cortex, anterolateral part

VISam, Visual cortex, anteromedial part

VISl, Visual cortex, lateral part

VISp, Visual cortex, primary

VISpl, Visual cortex, posterolateral part

VISpm, Visual cortex, posteromedial part

VM, Ventromedial nucleus thalamus

vmPFC, Ventromedial prefrontal cortex

VMH, Ventromedial hypothalamic nucleus

VMH.c, Ventromedial hypothalamic nucleus, central part

VMH.dm, Ventromedial hypothalamic nucleus, dorsomedial part

VMH.vl, Ventromedial hypothalamic nucleus, ventrolateral part

ZI, Zona incerta

ZI.m, Zona incerta, medial part

ZI.c, Zona incerta, central part

ZI.l, Zona incerta, lateral part

Supplementary Table 2 | Injection Site List.

Injection site coordinates and tracer information for all cases used throughout the study. Cases are identified by Case ID, Injection Site (ROI, region of interest), Tracer, Tracer Type, Figure reference, ARA Level of injection site, and Coordinates for the injection site based on the Allen Reference Atlas Coordinate Frame. Cortex cases can be cross-referenced to flat map injection site location in Supplementary Figure 1 (n=44 mice with 86 total cortical pathways).

| Cortex cases with anterograde projections to Superior Colliculus | | | | | | | | | | | |
|--|-----------|----------------|----------------------|--------------|-----------------------|--------------------|-----------|--------|--------|--------|--|
| Mouse # | Pathway # | Case ID | Injection Site (ROI) | Tracer | Tracer Type | Figure | ARA Level | ML (X) | AP (Y) | DV (Z) | |
| 1 | 1 | SW110321-04B/A | ACAv interm | PHAL-488 | classic / anterograde | 3g, 4b | 56 | 0.4 | -0.18 | -0.75 | |
| 2 | 2 | SW110322-03A | MOs caudal | PHAL-488 | classic / anterograde | 2g, 4b | 58 | 0.6 | -0.38 | -0.75 | |
| 3 | 3 | SW110322-03A | SSp-ul | BDA | classic / anterograde | 4b | 58 | 2.3 | -0.38 | -1.5 | |
| 3 | 4 | SW110516-02B/A | SSp-n | PHAL-488 | classic / anterograde | 2g, 4b | 50 | 3.1 | 0.45 | -2.7 | |
| 4 | 5 | SW110613-03B/A | RSPd rostral | PHAL-488 | classic / anterograde | 3b, SF4a, 4b | 83 | 0.6 | -2.98 | -0.25 | |
| 5 | 6 | SW110614-03B/A | RSPd caudal | PHAL-488 | classic / anterograde | 4b | 88 | 0.6 | -3.45 | -0.25 | |
| 6 | 7 | SW110615-01B/A | RSPagl | PHAL-488 | classic / anterograde | 3b, 3g, 4b | 91 | 0.9 | -3.78 | -0.25 | |
| 7 | 8 | SW110615-03B/A | RSPv rostral | PHAL-488 | classic / anterograde | 3b, SF4a, 4b | 73 | 0.5 | -1.85 | -0.75 | |
| 8 | 9 | SW110808-02A | ORBl | PHAL-488 | classic / anterograde | SF4b, 4b | 37 | 1.75 | 1.95 | -3.25 | |
| 9 | 10 | SW110808-04A | ORBm | PHAL-488 | classic / anterograde | 3b, 4b | 28 | 0.6 | 2.62 | -2.4 | |
| 10 | 11 | SW120125-01A | TEa rostral | PHAL-488 | classic / anterograde | 3b, 4b | 78 | 4.25 | -2.35 | -3.4 | |
| 11 | 12 | SW120403-02A | ACAv rostral | PHAL-488 | classic / anterograde | 3b, SF4a, 4b | 44 | 0.5 | 1.05 | -1.8 | |
| 12 | 13 | SW120819-04A | VISI | BDA | classic / anterograde | 4b | 92 | 3.5 | -3.88 | -1.75 | |
| 12 | 14 | SW120819-04A | TEa caudal | PHAL-488 | classic / anterograde | 3b, 4b | 94 | 4.1 | -4.08 | -2.5 | |
| 13 | 15 | SW121031-03B/A | SSp-tr/l | AAV-tdTomato | virus / anterograde | 4b | 70 | 1.6 | -1.55 | -0.75 | |
| 16 | 16 | SW121031-03B/A | ACAd interm | PHAL-647 | classic / anterograde | 3b, SF4a, 4b | 46 | 0.4 | 0.85 | 1.25 | |
| 17 | 17 | SW121031-03B/A | VISam | AAV-GFP | virus / anterograde | 4b | 83 | 1.6 | -2.98 | -0.5 | |
| 14 | 18 | SW121031-04B/A | ACAv interm | PHAL-647 | classic / anterograde | 3b, 4b | 54 | 0.4 | 0.2 | -1.6 | |
| 19 | 19 | SW121031-04B/A | SSp-tr | AAV-tdTomato | virus / anterograde | 2f, 4b | 74 | 2 | -1.98 | -1 | |
| 20 | 20 | SW121031-04B/A | AUDp interm | AAV-GFP | virus / anterograde | 2g, 2f, 3g, 4b | 84 | 4.1 | -3.1 | -2.5 | |
| 15 | 21 | SW121210-02A | MOs medial | AAV-GFP | virus / anterograde | 2g, 4b | 49 | 0.5 | 0.55 | -0.85 | |
| 16 | 22 | SW121221-02A | VISp caudolat | BDA | classic / anterograde | 4b | 96 | 2.75 | -4.28 | -1.25 | |
| 23 | 23 | SW121221-02A | VISp caudomed | PHAL-488 | classic / anterograde | 2g, 4b | 96 | 2.5 | -4.28 | -1 | |
| 17 | 24 | SW121221-03A | VISp caudal | BDA | classic / anterograde | 2g, 4b | 95 | 1.8 | -4.12 | -0.75 | |
| 25 | 25 | SW121221-03A | VISp rostral | PHAL-488 | classic / anterograde | 4b | 86 | 5 | -3.28 | -1.75 | |
| 18 | 26 | SW151210-01A | ACAd rostral | AAV-tdTomato | virus / anterograde | 3b, 3g, 4b | 36 | 0.3 | 1.85 | -1.25 | |
| 27 | 27 | SW151210-01A | SSs | AAV-GFP | virus / anterograde | 4b | 53 | 3.25 | 0.15 | -3.25 | |
| 19 | 28 | SW151210-02A | VISam | AAV-tdTomato | virus / anterograde | 3c, 3g, 4b | 84 | 1.5 | -3.08 | -0.75 | |
| 29 | 29 | SW151210-02A | SSp-tr | AAV-GFP | virus / anterograde | 3c, 4b | 74 | 2 | -1.95 | -0.7 | |
| 20 | 30 | SW151211-01A/B | VISp | AAV-GFP | virus / anterograde | 3d, 6a, 4b | 92 | 3 | -3.88 | -1.2 | |
| 31 | 31 | SW151211-01A/B | ACAd rostral | AAV-tdTomato | virus / anterograde | 3b, 3d, 6a, 4b | 37 | 0.6 | -1.75 | -1.25 | |
| 32 | 32 | SW151211-01A/B | RSPv caudal | PHAL-647 | classic / anterograde | 3b, 3d, 3g, 6a, 4b | 90 | 0.5 | -3.68 | -0.75 | |
| 21 | 33 | SW151211-02A | ACAd caudal | AAV-tdTomato | virus / anterograde | 3c, 4b | 58 | 0.4 | -0.38 | -1 | |
| 34 | 34 | SW151211-02A | VISam | PHAL-647 | classic / anterograde | 3c, 4b | 86 | 1.5 | -3.28 | -0.5 | |
| 35 | 35 | SW151211-02A | SSp-tr | AAV-GFP | virus / anterograde | 3c, 4b | 76 | 3 | -2.15 | -1.2 | |
| 22 | 36 | SW151215-03A | PTLp lat | AAV-tdTomato | virus / anterograde | 3b, 4b | 82 | 3.6 | -2.88 | -1.75 | |
| 23 | 37 | SW170410-03A | SSp-II | AAV-GFP | virus / anterograde | 3g, 4b | 56 | 2.2 | -0.18 | -1.25 | |
| 38 | 38 | SW170410-03A | SSp-ul | AAV-tdTomato | virus / anterograde | 3g, 4b | 47 | 2.5 | -0.75 | 1.5 | |
| 24 | 39 | SW170410-04A | SSp-m | AAV-tdTomato | virus / anterograde | 3g, 4b, SF3c | 43 | 2.75 | 1.15 | -2.5 | |
| 40 | 40 | SW170410-04A | SSp-ul | AAV-GFP | virus / anterograde | 4b, SF3c | 49 | 2.5 | 0.55 | -1.5 | |
| 25 | 41 | SW171101-01A | MOp-oro | PHAL-647 | classic / anterograde | 3g, 4b | 34 | 2.1 | 2.1 | -2.75 | |
| 42 | 42 | SW171101-01A | MOp-ul | AAV-tdTomato | virus / anterograde | 4b | 44 | 1.5 | 1.1 | -1.5 | |
| 43 | 43 | SW171101-01A | MOp-bfd | AAV-GFP | virus / anterograde | 3g, 4b | 38 | 1.8 | 1.65 | -1.4 | |
| 26 | 44 | SW171130-02A | MOs lateral | AAV-tdTomato | virus / anterograde | 2d, 4b | 44 | 1.1 | 1.1 | -1.5 | |
| 45 | 45 | SW171130-02A | MOs lateral | AAV-GFP | virus / anterograde | 2d, 4b | 46 | 1.1 | 0.85 | -1.25 | |
| 46 | 46 | SW171130-02A | MOp-oro | PHAL-647 | classic / anterograde | 2d, 4b | 40 | 1.4 | 1.42 | -1.6 | |
| 27 | 47 | SW180117-01A | ORBl | PHAL-647 | classic / anterograde | 3b, 4b | 35 | 1.5 | 2.1 | -3.3 | |
| 48 | 48 | SW180117-01A | MOp-oro | AAV-tdTomato | virus / anterograde | 3g, 4b | 35 | 1.5 | 2.1 | -1.75 | |
| 49 | 49 | SW180117-01A | MOp-ul | AAV-GFP | virus / anterograde | 3g, 4b | 41 | 1.4 | 1.35 | -1.4 | |
| 28 | 50 | SW180227-01A | ACAd interm | PHAL-647 | classic / anterograde | 3g, 4b | 42 | 0.5 | 1.25 | -1.4 | |
| 51 | 51 | SW180227-01A | MOs medial | AAV-tdTomato | virus / anterograde | 3g, 4b | 40 | 0.6 | 1.42 | -1.25 | |
| 29 | 52 | SW180227-02A | ACAd interm | PHAL-647 | classic / anterograde | 4b | 47 | 0.3 | 0.75 | -1.2 | |
| 53 | 53 | SW180227-02A | MOs medial | AAV-tdTomato | virus / anterograde | 4b | 47 | 0.4 | 0.75 | -0.75 | |
| 30 | 54 | SW180228-03A | ACAv caudal | AAV-tdTomato | virus / anterograde | 3b, 4b | 58 | 0.4 | -0.38 | -1.25 | |
| 55 | 55 | SW180302-04A | VISal | AAV-tdTomato | virus / anterograde | 4b | 91 | 3.4 | -3.88 | -1.6 | |
| 56 | 56 | SW180302-04A | PTLp lat | AAV-GFP | virus / anterograde | 4b | 82 | 3.5 | -2.88 | -1.65 | |
| 31 | 57 | SW180302-05A | VISp caudolat | PHAL-647 | classic / anterograde | 2c, 4b | 94 | 2.25 | -3.88 | -1 | |
| 58 | 58 | SW180302-05A | VISal | AAV-tdTomato | virus / anterograde | 2c, 4b | 90 | 3.4 | -3.68 | -1.3 | |
| 59 | 59 | SW180302-05A | PTLp lat | AAV-GFP | virus / anterograde | 2c, 4b | 81 | 3.6 | -2.88 | -1.75 | |
| 32 | 60 | SW180424-01A | PTLp med | AAV-tdTomato | virus / anterograde | 3b, 4b | 77 | 2.25 | -2.55 | -6 | |
| 61 | 61 | SW180424-01A | PTLp med | PHAL-488 | classic / anterograde | 3g, 4b | 77 | 1.5 | -2.55 | -6 | |
| 33 | 62 | SW180516-02A | MOp-oro | PHAL-647 | classic / anterograde | 4b | 32 | 2 | 2.25 | -2.5 | |
| 63 | 63 | SW180516-02A | MOp-bfd | AAV-tdTomato | virus / anterograde | 4b | 40 | 1.6 | 1.42 | -1.6 | |
| 64 | 64 | SW180516-02A | MOp-tr | AAV-GFP | virus / anterograde | 4b | 52 | 1.6 | 0.25 | -1.3 | |
| 34 | 65 | SW180522-04A | VISI/pl | AAV-tdTomato | virus / anterograde | 4b | 97 | 3.5 | -4.15 | -2 | |
| 35 | 66 | SW180713-03A | VISp | AAV-tdTomato | virus / anterograde | 4b | 90 | 2 | -3.98 | -0.8 | |
| 67 | 67 | SW180713-03A | SSp-tr | PHAL-647 | classic / anterograde | 4b | 68 | 2 | -1.35 | -1.25 | |
| 68 | 68 | SW180713-03A | AUDd | AAV-GFP | virus / anterograde | 3g | 74 | 4 | -1.95 | -2.1 | |
| 36 | 69 | SW180713-04A | VISp rostromed | AAV-GFP | virus / anterograde | 3g, 6a, 4b | 87 | 2.25 | -3.38 | -0.75 | |
| 70 | 70 | SW180713-04A | SSp-tr | AAV-tdTomato | virus / anterograde | 4b, 6a, SF3c | 68 | 2.5 | -1.35 | -1.25 | |
| 71 | 71 | SW180713-04A | AUDd | PHAL-647 | classic / anterograde | 4b, 6a | 74 | 4 | -1.95 | -2.1 | |
| 37 | 72 | SW180717-03A | PTLp med | PHAL-488 | classic / anterograde | 3f, 4b | 76 | 1.25 | -2.15 | -0.6 | |
| 73 | 73 | SW180717-03A | PTLp med | AAV-tdTomato | virus / anterograde | 3f, 4b | 76 | 2.1 | -2.15 | -0.75 | |
| 38 | 74 | SW180815-01A | VISI | AAV-tdTomato | virus / anterograde | 3g, 4b | 92 | 3.75 | -3.88 | -2 | |
| 39 | 75 | SW181109-09A | SSp-bfd | AAV-GFP | virus / anterograde | 4b, SF3c | 64 | 3 | -0.95 | -1.5 | |
| 76 | 76 | SW181109-09A | SSp-bfd | AAV-tdTomato | virus / anterograde | 4b, SF3c | 64 | 3.5 | -0.95 | -2 | |
| 40 | 77 | SW190315-05A | PL | AAV-tdTomato | virus / anterograde | 3b, 4b, 6a, SF4b | 33 | 0.4 | 2.15 | -2.3 | |
| 78 | 78 | SW190315-05A | MOs rostral | PHAL-647 | classic / anterograde | 2c, 4b, 6a | 31 | 1.3 | 2.35 | -1.5 | |
| 79 | 79 | SW190315-05A | MOp-oro | AAV-GFP | virus / anterograde | 2c, 4b, 6a | 31 | 2 | 2.35 | -3 | |
| 41 | 80 | SW190315-07A | ILA | PHAL-647 | classic / anterograde | 3b, 4b | 37 | 0.5 | 1.75 | -3 | |
| 42 | 81 | SW190315-09A | AUDp rostral | AAV-tdTomato | virus / anterograde | 4b | 76 | 4.1 | -2.15 | -2.6 | |
| 82 | 82 | SW190315-09A | AUDp caudal | AAV-GFP | virus / anterograde | 4b | 86 | 4.1 | -3.28 | -2.3 | |
| 83 | 83 | SW190315-09A | AUDv | PHAL-647 | classic / anterograde | 4b | 70 | 4.2 | -1.56 | -3.1 | |
| 43 | 84 | SW190327-02A | ORBvl | AAV-GFP | virus / anterograde | 3b, 3g, 4b, SF4b | 33 | 1.25 | 2.15 | -3.1 | |
| 44 | 85 | SW190327-04A | RSPv interm | AAV-GFP | virus / anterograde | 3b, 4b | 88 | 0.4 | -3.45 | -0.6 | |
| 86 | 86 | SW190327-04A | VISpm | AAV-tdTomato | virus / anterograde | 3g, 4b | 94 | 1.25 | -4.08 | -0.75 | |

(Supplementary Table 2 : Continued)

| Additional cases used throughout study | | | | | | | | | | | |
|--|-----------|--------------|----------------------|------------------------------|-----------------------|------------|-----------|--------|--------|--------|--|
| Mouse # | Pathway # | Case ID | Injection Site (ROI) | Tracer | Tracer Type | Figure | ARA Level | ML (X) | AP (Y) | DV (Z) | |
| 45 | 87 | SW150916-01A | SC.m | PHAL | classic / anterograde | 4b | 86 | 0.5 | -3.28 | -0.4 | |
| | 88 | SW150916-01A | SC.I | BDA | classic / anterograde | 4b | 86 | 1.1 | -3.28 | -2.5 | |
| | 89 | SW150916-01A | SC.m | CTB-555 | classic / retrograde | 4b | 86 | 0.5 | -3.28 | -0.4 | |
| | 90 | SW150916-01A | SC.I | FG | classic / retrograde | 4b | 86 | 1.1 | -3.28 | -2.5 | |
| 46 | 91 | SW150921-01A | SC.m | FG | classic / retrograde | 4b | 90 | 0.3 | -3.68 | -1.6 | |
| 47 | 92 | SW160716-01A | SC.cl/l | PHAL | classic / anterograde | 4b | 100 | 0.5 | -4.65 | -1.3 | |
| 48 | 93 | SW160716-02A | SC.cm | PHAL | classic / anterograde | 4b | 100 | 0.3 | -4.65 | -1.2 | |
| | 94 | SW160716-02A | SC.cm | FG | classic / retrograde | 4b | 86 | 0.5 | -3.28 | -2.3 | |
| 49 | 95 | SW170201-05A | SC.m-iw/dg | CTB-647 | classic / retrograde | 4b, 5a | 96 | 0.2 | -4.28 | -1.75 | |
| | 96 | SW170201-05A | SC.cl-dg | CTB-555 | classic / retrograde | 4b, 5a | 96 | 0.6 | -4.28 | -2.25 | |
| | 97 | SW170201-05A | SC.l-dg | CTB-488 | classic / retrograde | 4b, 5a | 96 | 0.9 | -4.28 | -2.6 | |
| 50 | 98 | SW170201-08A | SC.cm-iw/dg | CTB-555 | classic / retrograde | 4b, 5a | 96 | 0.6 | -4.28 | -1.5 | |
| | 99 | SW170201-08A | SC.l-ig | FG | classic / retrograde | 4b, 5a | 96 | 1.4 | -4.28 | -2.4 | |
| 51 | 100 | SW170215-01A | SC.cm | PHAL | classic / anterograde | 4b | 86 | 0.5 | -3.28 | -2.3 | |
| 52 | 101 | SW170315-01A | SC.cl/l | AAV-tdTomato | virus / anterograde | 4b | 90 | 1.5 | -3.68 | -2 | |
| 53 | 102 | SW170315-02A | SC.cm | CTB-647 | classic / retrograde | 4b | 90 | 0.5 | -3.68 | -1.5 | |
| | 103 | SW170315-02A | SC.cl | FG | classic / retrograde | 4b | 90 | 1.5 | -3.68 | -2.75 | |
| 54 | 104 | SW170426-04A | SC.I | AAV-tdTomato | virus / anterograde | 4b | 96 | 1.1 | -4.28 | -2.1 | |
| 55 | 105 | SW170830-01A | SC.m | CTB-647 | classic / retrograde | 4b | 100 | 0.3 | -4.65 | -1.5 | |
| 56 | 106 | SW170830-02A | SC.cm | CTB-647 | classic / retrograde | 4b | 100 | 0.25 | -4.65 | -1.3 | |
| | 107 | SW170830-02A | SC.cl | CTB-488 | classic / retrograde | 4b | 100 | 0.75 | -4.65 | -1.3 | |
| 57 | 108 | SW171010-01A | SC.l-ig/iw | AAV-tdTomato | virus / anterograde | 4a-b, SF6c | 90 | 1 | -3.68 | -2.8 | |
| | 109 | SW171010-01A | SC.l-dg | PHAL | virus / anterograde | 4a-b | 88 | 1.25 | -3.45 | -2.75 | |
| | 110 | SW171010-01A | SC.cl-dg | AAV-GFP | virus / anterograde | 4a-b | 94 | 1 | -4.08 | 2.5 | |
| 58 | 111 | SW171010-02A | SC.cm | AAV-tdTomato | virus / anterograde | 4a-b, SF6b | 90 | 0.55 | -3.68 | -2.4 | |
| | 112 | SW171010-02A | SC.cl | AAV-GFP | virus / anterograde | 4a-b, SF6b | 90 | 0.75 | -3.68 | -2.5 | |
| 59 | 113 | SW171010-03A | SC.m | AAV-tdTomato | virus / anterograde | 4b | 96 | 0.4 | -4.28 | -1.6 | |
| 60 | 114 | SW180614-07A | SC.m | AAV-tdTomato | virus / anterograde | 4b | 96 | 0.25 | -4.28 | -1.2 | |
| | 115 | SW180614-07A | SC.cl | AAV-GFP | virus / anterograde | 4b | 96 | 0.9 | -4.28 | -1.6 | |
| 61 | 116 | SW190619-02A | SC.m/cm | PHAL | classic / anterograde | 4a-b | 90 | 0.5 | -3.68 | -1.5 | |
| | 117 | SW190619-02A | SC.cl | AAV-tdTomato | virus / anterograde | 4a-b | 90 | 0.8 | -3.68 | -2.1 | |
| 62 | 118 | SW190619-04A | SC.m-iw/dg | PHAL | classic / anterograde | 4a-b, SF6a | 90 | 0.25 | -3.68 | -1.8 | |
| 63 | 119 | SW140603-01A | LD | FG | classic / retrograde | SF3a | 69 | 1.2 | -1.45 | -2.6 | |
| 64 | 120 | SW140603-03A | MD | FG | classic / retrograde | 5c | 66 | 0.3 | -1.15 | -3.2 | |
| 65 | 121 | SW140916-04A | RE | FG | classic / retrograde | 5c | 61 | 0.2 | -0.65 | -4.7 | |
| 66 | 122 | SW141021-02A | LP | FG | classic / retrograde | SF3a | 77 | 1.6 | -2.25 | -2.5 | |
| 67 | 123 | SW150716-02A | SNr.cl | PHAL-488 | classic / anterograde | 5d | 84 | 1.2 | -3.08 | -5.2 | |
| 68 | 124 | SW171002-03A | SNr.I | PHAL-647 | classic / anterograde | 5d | 84 | 1 | -3.08 | -5.25 | |
| | 125 | SW171002-03A | SNr.dl | AAV-RFP | classic / anterograde | 5d | 84 | 1.5 | -3.08 | -5.1 | |
| | 126 | SW171002-03A | SNr.dn | AAV-GFP | classic / anterograde | 5d | 84 | 0.75 | -3.08 | -5.3 | |
| 69 | 127 | SW171213-02A | PF.m | FG | classic / retrograde | 5c | 75 | 0.7 | -2.05 | -3.75 | |
| 70 | 128 | SW180508-04A | SNr.v | PHAL-647 | classic / anterograde | 5e | 84 | 1.5 | -3.08 | -5.5 | |
| | 129 | SW180508-04A | SNr.dl | AAV-tdTomato | classic / anterograde | 5e | 84 | 1.5 | -3.08 | -5.1 | |
| | 130 | SW180508-04A | SNr.dn | AAV-GFP | classic / anterograde | 5e | 84 | 1 | -3.08 | -5.5 | |
| 71 | 131 | SW190110-01B | CPc,dm | AAVretro-EF1a-Cre | virus / retrograde | 6b | 57 | 1.6 | -0.28 | -2.5 | |
| | 132 | SW190110-01B | MOs | AAV1LCAG-FLEX-tdTom | virus / anterograde | 6b | 47 | 0.5 | 0.75 | -1 | |
| 72 | 133 | SW190207-09A | SNr.m | AAV-RFP | virus / anterograde | 5d | 84 | 0.75 | -3.08 | -5.6 | |
| 73 | 134 | SW190213-01A | VM/PCN | FG | classic / retrograde | SF3a | 72 | 0.6 | -1.75 | -4 | |
| 74 | 135 | SW190829-03A | ZI.medial | AAV-RFP | virus / anterograde | 5b | 74 | 0.6 | -1.95 | -5 | |
| 75 | 136 | SW190926-10 | PF.ul | AAVretro-EF1a-Cre | virus / retrograde | 7, 4b | 75 | 0.5 | -2.05 | -3.4 | |
| | 137 | SW190926-10 | SC.l-ig | iSyn-FLEX-TVA-P2A-GFP | virus / anterograde | 7, 4b | 90 | 1.5 | -3.68 | -2.5 | |
| | 138 | SW190926-10 | SC.l-ig | nvA G-deleted-rabies-mCherry | virus / retrograde | 7, 4b | 90 | 1.5 | -3.68 | -2.5 | |
| 76 | 139 | SW191011-01A | ZI.lateral | PHAL-647 | classic / anterograde | 5b | 71 | 1.75 | -1.65 | -4.5 | |
| 77 | 140 | SW191011-02A | ZI.central | PHAL-647 | classic / anterograde | 5b | 74 | 1.25 | -1.95 | -4.3 | |

| Cortex regions which do not send anterograde projections to Superior Colliculus | | | | | | | | | | | |
|---|-----|--------------|-------|--------------|-----------------------|-----|-----|------|-------|-------|--|
| 78 | 141 | SW121220-05A | Ald | BDA | classic / anterograde | n/a | 31 | 2.5 | 2.35 | -3.75 | |
| 79 | 142 | SW120403-01A | Ald | BDA | classic / anterograde | n/a | 27 | 2.3 | 2.75 | -3.75 | |
| 80 | 143 | SW110321-04B | Alp | BDA | classic / anterograde | n/a | 56 | 4.1 | -0.18 | -4.6 | |
| 81 | 144 | SW110906-02A | Alp | PHAL-488 | classic / anterograde | n/a | 64 | 4.3 | -0.95 | -4.5 | |
| 82 | 145 | SW120118-01A | Ald/v | BDA | classic / anterograde | n/a | 44 | 3.4 | 1.05 | -4.5 | |
| 83 | 146 | SW110906-02A | GU | PHAL-488 | classic / anterograde | n/a | 38 | 2.9 | 1.65 | -3.5 | |
| 84 | 147 | SW120125-03A | GU | PHAL-488 | classic / anterograde | n/a | 37 | 2.75 | 1.75 | -3.3 | |
| 85 | 148 | SW110905-01A | VISC | BDA | classic / anterograde | n/a | 54 | 4 | 0.02 | -4.1 | |
| 86 | 149 | SW120118-02A | VISC | BDA | classic / anterograde | n/a | 66 | 4.4 | -1.15 | -4 | |
| 87 | 150 | SW110906-04A | ECT | BDA | classic / anterograde | n/a | 84 | 4.4 | -3.08 | -3.95 | |
| 88 | 151 | SW180815-02A | ENT | AAV-tdTomato | virus / anterograde | n/a | 101 | 4.75 | -4.78 | -2.75 | |
| 89 | 152 | SW120403-03A | PERI | BDA | classic / anterograde | n/a | 87 | 4.7 | -3.38 | -3.9 | |

Supplementary Table 3 | Proportion of labeling values: sensory cortex ROIs to SC zones-layers.

Values represent proportion of pixel density for the selected ROI (n=1 per cortical area) distributed across each SC zone across all layers. Far right summations correspond to values used in Figure 2g.

| | SC.m | | | | | | SC.cm | | | | | | SC.cl | | | | | | SC.I | | | | | | Summations | | | | | | | |
|----------------|---------|---------|---------|---------|---------|---------|---------|----------|----------|----------|----------|----------|----------|----------|----------|----------|----------|----------|----------|----------|----------|---------|---------|---------|------------|------|-------|-------|------|------|------|------|
| | SC.m-zo | SC.m-sg | SC.m-op | SC.m-ig | SC.m-iw | SC.m-dg | SC.m-dw | SC.cm-zo | SC.cm-sg | SC.cm-op | SC.cm-ig | SC.cm-iw | SC.cm-dg | SC.cm-dw | SC.cl-zo | SC.cl-sg | SC.cl-op | SC.cl-ig | SC.cl-iw | SC.cl-dg | SC.cl-dw | SC.l-ig | SC.l-iw | SC.l-dg | SC.l-dw | SC.m | SC.cm | SC.cl | SC.I | | | |
| VISp caudal | 0.45 | 0.57 | 0.08 | 0.00 | 0.00 | 0.00 | 0.00 | 0.05 | 0.01 | 0.00 | 0.00 | 0.00 | 0.00 | 0.00 | 0.00 | 0.00 | 0.00 | 0.00 | 0.00 | 0.00 | 0.00 | 0.00 | 0.00 | 0.00 | 0.00 | 0.00 | 0.00 | 0.00 | | | | |
| VISam | 0.00 | 0.04 | 0.13 | 0.22 | 0.09 | 0.03 | 0.00 | 0.00 | 0.07 | 0.15 | 0.13 | 0.07 | 0.03 | 0.02 | 0.00 | 0.02 | 0.07 | 0.02 | 0.02 | 0.01 | 0.02 | 0.00 | 0.00 | 0.00 | 0.00 | 0.02 | 0.00 | 0.00 | | | | |
| VISal | 0.00 | 0.10 | 0.12 | 0.04 | 0.00 | 0.00 | 0.01 | 0.34 | 0.50 | 0.05 | 0.00 | 0.00 | 0.00 | 0.00 | 0.00 | 0.01 | 0.00 | 0.00 | 0.00 | 0.00 | 0.00 | 0.00 | 0.00 | 0.00 | 0.00 | 0.00 | 0.00 | 0.00 | | | | |
| VISp caudomed | 0.00 | 0.02 | 0.03 | 0.01 | 0.00 | 0.00 | 0.00 | 0.22 | 0.53 | 0.30 | 0.04 | 0.00 | 0.00 | 0.00 | 0.00 | 0.01 | 0.00 | 0.00 | 0.00 | 0.00 | 0.00 | 0.00 | 0.00 | 0.00 | 0.00 | 0.00 | 0.00 | 0.00 | | | | |
| VISp rostromed | 0.00 | 0.00 | 0.00 | 0.00 | 0.00 | 0.00 | 0.00 | 0.05 | 0.13 | 0.13 | 0.03 | 0.00 | 0.00 | 0.00 | 0.00 | 0.19 | 0.44 | 0.20 | 0.02 | 0.00 | 0.00 | 0.00 | 0.00 | 0.00 | 0.00 | 0.00 | 0.00 | 0.00 | | | | |
| AUDp interm | 0.00 | 0.00 | 0.00 | 0.00 | 0.13 | 0.07 | 0.00 | 0.00 | 0.00 | 0.07 | 0.20 | 0.35 | 0.05 | 0.00 | 0.00 | 0.00 | 0.06 | 0.07 | 0.02 | 0.13 | 0.00 | 0.02 | 0.00 | 0.00 | 0.00 | 0.00 | 0.00 | 0.00 | | | | |
| MOs medial | 0.00 | 0.00 | 0.02 | 0.06 | 0.06 | 0.01 | 0.01 | 0.00 | 0.03 | 0.08 | 0.05 | 0.01 | 0.01 | 0.00 | 0.01 | 0.03 | 0.13 | 0.15 | 0.07 | 0.06 | 0.03 | 0.06 | 0.08 | 0.21 | 0.00 | 0.00 | 0.00 | 0.00 | | | | |
| SSp tr | 0.00 | 0.00 | 0.01 | 0.06 | 0.04 | 0.00 | 0.00 | 0.00 | 0.00 | 0.15 | 0.05 | 0.00 | 0.00 | 0.00 | 0.02 | 0.25 | 0.21 | 0.07 | 0.01 | 0.12 | 0.08 | 0.08 | 0.00 | 0.11 | 0.20 | 0.56 | 0.28 | 0.00 | 0.00 | | | |
| AUDd | 0.00 | 0.00 | 0.02 | 0.04 | 0.00 | 0.00 | 0.00 | 0.00 | 0.00 | 0.18 | 0.03 | 0.00 | 0.00 | 0.00 | 0.00 | 0.00 | 0.19 | 0.13 | 0.06 | 0.00 | 0.09 | 0.24 | 0.18 | 0.00 | 0.06 | 0.21 | 0.38 | 0.51 | 0.00 | 0.00 | | |
| MOs caudal | 0.00 | 0.00 | 0.00 | 0.02 | 0.01 | 0.01 | 0.02 | 0.00 | 0.00 | 0.01 | 0.03 | 0.01 | 0.02 | 0.00 | 0.00 | 0.05 | 0.12 | 0.14 | 0.08 | 0.06 | 0.04 | 0.07 | 0.07 | 0.42 | 0.00 | 0.02 | 0.45 | 0.60 | 0.00 | 0.00 | | |
| MOs lateral | 0.00 | 0.00 | 0.00 | 0.00 | 0.00 | 0.00 | 0.00 | 0.00 | 0.00 | 0.02 | 0.00 | 0.00 | 0.00 | 0.00 | 0.00 | 0.07 | 0.26 | 0.10 | 0.01 | 0.00 | 0.25 | 0.18 | 0.10 | 0.18 | 0.00 | 0.00 | 0.02 | 0.01 | 0.00 | 0.00 | | |
| SSp bfld | 0.00 | 0.00 | 0.00 | 0.00 | 0.00 | 0.00 | 0.00 | 0.00 | 0.00 | 0.00 | 0.00 | 0.00 | 0.00 | 0.00 | 0.00 | 0.00 | 0.25 | 0.06 | 0.00 | 0.00 | 0.51 | 0.30 | 0.05 | 0.00 | 0.00 | 0.00 | 0.00 | 0.00 | 0.00 | 0.00 | 0.00 | |
| MOp-tr | 0.00 | 0.00 | 0.00 | 0.00 | 0.00 | 0.00 | 0.00 | 0.00 | 0.00 | 0.00 | 0.00 | 0.00 | 0.00 | 0.00 | 0.01 | 0.00 | 0.24 | 0.11 | 0.02 | 0.00 | 0.00 | 0.66 | 0.04 | 0.09 | 0.00 | 0.00 | 0.00 | 0.00 | 0.00 | 0.00 | 0.00 | |
| MOs rostral | 0.00 | 0.00 | 0.00 | 0.00 | 0.00 | 0.00 | 0.00 | 0.00 | 0.00 | 0.00 | 0.00 | 0.00 | 0.00 | 0.00 | 0.00 | 0.01 | 0.07 | 0.00 | 0.00 | 0.00 | 0.00 | 0.81 | 0.19 | 0.08 | 0.00 | 0.00 | 0.00 | 0.00 | 0.00 | 0.00 | 0.00 | |
| SSp ll | 0.00 | 0.00 | 0.00 | 0.00 | 0.00 | 0.00 | 0.00 | 0.00 | 0.00 | 0.00 | 0.00 | 0.00 | 0.00 | 0.00 | 0.00 | 0.00 | 0.02 | 0.06 | 0.01 | 0.00 | 0.00 | 0.50 | 0.27 | 0.32 | 0.00 | 0.00 | 0.00 | 0.00 | 0.00 | 0.00 | 0.00 | 0.00 |
| MOp-oro | 0.00 | 0.00 | 0.00 | 0.00 | 0.00 | 0.00 | 0.00 | 0.00 | 0.00 | 0.00 | 0.00 | 0.00 | 0.00 | 0.00 | 0.00 | 0.00 | 0.05 | 0.01 | 0.00 | 0.00 | 0.00 | 0.50 | 0.54 | 0.07 | 0.00 | 0.00 | 0.00 | 0.00 | 0.00 | 0.00 | 0.00 | 0.00 |
| SSp m | 0.00 | 0.00 | 0.00 | 0.00 | 0.00 | 0.00 | 0.00 | 0.00 | 0.00 | 0.00 | 0.00 | 0.00 | 0.00 | 0.00 | 0.00 | 0.00 | 0.00 | 0.00 | 0.00 | 0.00 | 0.00 | 0.82 | 0.32 | 0.02 | 0.00 | 0.00 | 0.00 | 0.00 | 0.00 | 0.00 | 0.00 | 0.00 |
| SSp n | 0.00 | 0.00 | 0.00 | 0.00 | 0.00 | 0.00 | 0.00 | 0.00 | 0.00 | 0.00 | 0.00 | 0.00 | 0.00 | 0.00 | 0.00 | 0.00 | 0.00 | 0.00 | 0.00 | 0.00 | 0.00 | 0.81 | 0.32 | 0.04 | 0.00 | 0.00 | 0.00 | 0.00 | 0.00 | 0.00 | 0.00 | 0.00 |
| SSp ul | 0.00 | 0.00 | 0.00 | 0.00 | 0.00 | 0.00 | 0.00 | 0.00 | 0.00 | 0.00 | 0.00 | 0.00 | 0.00 | 0.00 | 0.00 | 0.00 | 0.00 | 0.00 | 0.00 | 0.00 | 0.00 | 0.64 | 0.39 | 0.14 | 0.00 | 0.00 | 0.00 | 0.00 | 0.00 | 0.00 | 0.00 | 0.00 |
| SSs | 0.00 | 0.00 | 0.00 | 0.00 | 0.00 | 0.00 | 0.00 | 0.00 | 0.00 | 0.00 | 0.00 | 0.00 | 0.00 | 0.00 | 0.00 | 0.00 | 0.00 | 0.00 | 0.00 | 0.00 | 0.00 | 0.89 | 0.25 | 0.03 | 0.00 | 0.00 | 0.00 | 0.00 | 0.00 | 0.00 | 0.00 | 0.00 |

Supplementary Table 4 | Proportion of labeling values: higher order cortex ROIs to SC zones-layers.

Values represent proportion of pixel density for the selected ROI (n=1 per cortical area) distributed across each SC zone across all layers. Far right summations correspond to values used in Figure 3b.

| | SC.m | | | | | | SC.cm | | | | | | SC.cl | | | | | | SC.I | | | | | | Summations | | | | | | | | | | |
|--------------|---------|---------|---------|---------|---------|---------|---------|----------|----------|----------|----------|----------|----------|----------|----------|----------|----------|----------|----------|----------|----------|---------|---------|---------|------------|------|-------|-------|------|------|------|------|------|------|------|
| | SC.m-zo | SC.m-sg | SC.m-op | SC.m-ig | SC.m-iw | SC.m-dg | SC.m-dw | SC.cm-zo | SC.cm-sg | SC.cm-op | SC.cm-ig | SC.cm-iw | SC.cm-dg | SC.cm-dw | SC.cl-zo | SC.cl-sg | SC.cl-op | SC.cl-ig | SC.cl-iw | SC.cl-dg | SC.cl-dw | SC.l-ig | SC.l-iw | SC.l-dg | SC.l-dw | SC.m | SC.cm | SC.cl | SC.I | | | | | | |
| RSPv caudal | 0.01 | 0.14 | 0.40 | 0.25 | 0.51 | 0.25 | 0.04 | 0.00 | 0.04 | 0.16 | 0.11 | 0.21 | 0.03 | 0.04 | 0.00 | 0.01 | 0.01 | 0.02 | 0.01 | 0.01 | 0.05 | 0.00 | 0.00 | 0.00 | 0.00 | 0.00 | 0.00 | 0.00 | 0.00 | 0.00 | 0.00 | | | | |
| RSPv intern | 0.05 | 0.28 | 0.57 | 0.49 | 0.19 | 0.04 | 0.00 | 0.05 | 0.10 | 0.22 | 0.18 | 0.03 | 0.02 | 0.03 | 0.00 | 0.01 | 0.01 | 0.02 | 0.00 | 0.00 | 0.00 | 0.00 | 0.00 | 0.00 | 0.00 | 0.00 | 0.00 | 0.00 | 0.00 | 0.00 | 0.00 | | | | |
| RSPd rostral | 0.00 | 0.06 | 0.30 | 0.41 | 0.33 | 0.06 | 0.05 | 0.00 | 0.02 | 0.15 | 0.23 | 0.30 | 0.05 | 0.03 | 0.00 | 0.03 | 0.01 | 0.07 | 0.02 | 0.04 | 0.00 | 0.00 | 0.01 | 0.16 | 0.00 | 0.00 | 0.00 | 0.00 | 0.00 | 0.00 | 0.00 | 0.00 | 0.00 | | |
| RSPd caudal | 0.00 | 0.04 | 0.13 | 0.22 | 0.27 | 0.08 | 0.00 | 0.02 | 0.12 | 0.25 | 0.26 | 0.43 | 0.22 | 0.13 | 0.00 | 0.01 | 0.03 | 0.00 | 0.03 | 0.01 | 0.08 | 0.00 | 0.00 | 0.00 | 0.00 | 0.00 | 0.00 | 0.00 | 0.00 | 0.00 | 0.00 | 0.00 | | | |
| RSPagl | 0.00 | 0.02 | 0.09 | 0.34 | 0.37 | 0.09 | 0.05 | 0.00 | 0.05 | 0.18 | 0.28 | 0.23 | 0.26 | 0.19 | 0.00 | 0.00 | 0.01 | 0.01 | 0.01 | 0.04 | 0.08 | 0.00 | 0.00 | 0.00 | 0.00 | 0.00 | 0.00 | 0.00 | 0.00 | 0.00 | 0.00 | 0.00 | | | |
| PTLp lat | 0.00 | 0.02 | 0.26 | 0.58 | 0.04 | 0.00 | 0.00 | 0.01 | 0.12 | 0.75 | 0.07 | 0.00 | 0.00 | 0.00 | 0.01 | 0.09 | 0.17 | 0.08 | 0.01 | 0.01 | 0.04 | 0.02 | 0.05 | 0.00 | 0.00 | 0.00 | 0.00 | 0.00 | 0.00 | 0.00 | 0.00 | 0.00 | 0.00 | | |
| TFa caudal | 0.00 | 0.01 | 0.06 | 0.08 | 0.46 | 0.25 | 0.09 | 0.00 | 0.01 | 0.02 | 0.14 | 0.21 | 0.39 | 0.16 | 0.00 | 0.00 | 0.03 | 0.02 | 0.18 | 0.23 | 0.01 | 0.00 | 0.00 | 0.00 | 0.00 | 0.00 | 0.00 | 0.00 | 0.00 | 0.00 | 0.00 | 0.00 | | | |
| ACAv caudal | 0.00 | 0.00 | 0.05 | 0.30 | 0.01 | 0.02 | 0.01 | 0.00 | 0.00 | 0.16 | 0.38 | 0.27 | 0.21 | 0.06 | 0.00 | 0.02 | 0.08 | 0.06 | 0.28 | 0.09 | 0.11 | 0.00 | 0.00 | 0.01 | 0.23 | 0.00 | 0.00 | 0.00 | 0.00 | 0.00 | 0.00 | 0.00 | 0.00 | 0.00 | 0.00 |
| ACAv intern | 0.00 | 0.01 | 0.05 | 0.14 | 0.13 | 0.10 | 0.14 | 0.00 | 0.01 | 0.05 | 0.20 | 0.26 | 0.20 | 0.32 | 0.00 | 0.01 | 0.03 | 0.04 | 0.08 | 0.14 | 0.23 | 0.00 | 0.00 | 0.03 | 0.16 | 0.00 | 0.00 | 0.00 | 0.00 | 0.00 | 0.00 | 0.00 | 0.00 | 0.00 | 0.00 |
| ACAv rostral | 0.00 | 0.00 | 0.02 | 0.08 | 0.15 | 0.18 | 0.15 | 0.00 | 0.00 | 0.01 | 0.11 | 0.28 | 0.26 | 0.25 | 0.00 | 0.00 | 0.01 | 0.05 | 0.14 | 0.19 | 0.38 | 0.00 | 0.01 | 0.05 | 0.01 | 0.00 | 0.00 | 0.00 | 0.00 | 0.00 | 0.00 | 0.00 | 0.00 | 0.00 | |
| RSPv rostral | 0.00 | 0.00 | 0.02 | 0.05 | 0.01 | 0.03 | 0.00 | 0.00 | 0.00 | 0.05 | 0 | | | | | | | | | | | | | | | | | | | | | | | | |

Supplementary Table 5 | Morphometric *p*-values.

Table of pairwise comparisons using the Wilcoxon rank sum test. Adjustments for *p*-value were made for multiple comparisons using the false discovery rate (fdr) method. *P*-values are listed for the following neuronal morphometric parameters: contraction, width, number of bifurcations, branch path length, fractal dimension, fragmentation, height, number of branches, and height/width ratio.

| Contraction | | | | | | | | |
|------------------------|---------------|-----------|-----------|----------------|------------|------------|----------------|------------|
| | PF/MPT - SC.m | RE - SC.m | LD - SC.m | PF/MPT - SC.cm | RE - SC.cm | LD - SC.cm | PF/MPT - SC.cl | RE - SC.cl |
| RE - SC.m | 0.0019 | - | - | - | - | - | - | - |
| LD - SC.m | 0.024 | 0.5253 | - | - | - | - | - | - |
| PF/MPT - SC.cm | 0.9578 | 0.0064 | 0.049 | - | - | - | - | - |
| RE - SC.cm | 0.1386 | 0.052 | 0.1172 | 0.2261 | - | - | - | - |
| LD - SC.cm | 0.1439 | 0.4747 | 0.2057 | 0.1412 | 0.5471 | - | - | - |
| PF/MPT - SC.cl | 0.2981 | 0.0019 | 0.0503 | 0.5471 | 0.0166 | 0.093 | - | - |
| RE - SC.cl | 0.4555 | 0.1386 | 0.4747 | 0.553 | 0.7076 | 0.7261 | 0.1439 | - |
| PF/MPT - SC.I | 0.4946 | 0.0064 | 0.052 | 0.7226 | 0.052 | 0.093 | 0.82 | 0.2981 |
| Width | | | | | | | | |
| | PF/MPT - SC.m | RE - SC.m | LD - SC.m | PF/MPT - SC.cm | RE - SC.cm | LD - SC.cm | PF/MPT - SC.cl | RE - SC.cl |
| RE - SC.m | 0.0058 | - | - | - | - | - | - | - |
| LD - SC.m | 0.2038 | 0.00068 | - | - | - | - | - | - |
| PF/MPT - SC.cm | 0.0844 | 0.2038 | 0.01633 | - | - | - | - | - |
| RE - SC.cm | 0.00057 | 0.03547 | 0.00057 | 0.01554 | - | - | - | - |
| LD - SC.cm | 0.73327 | 0.00738 | 0.03547 | 0.02743 | 0.00057 | - | - | - |
| PF/MPT - SC.cl | 0.00134 | 0.01633 | 0.00719 | 0.01518 | 0.35848 | 0.00719 | - | - |
| RE - SC.cl | 0.00599 | 0.00668 | 0.03547 | 0.01633 | 0.0058 | 0.03547 | 0.04028 | - |
| PF/MPT - SC.I | 0.00266 | 0.00057 | 0.02381 | 0.00917 | 0.00188 | 0.02381 | 0.00899 | 0.2038 |
| Number of Bifurcations | | | | | | | | |
| | PF/MPT - SC.m | RE - SC.m | LD - SC.m | PF/MPT - SC.cm | RE - SC.cm | LD - SC.cm | PF/MPT - SC.cl | RE - SC.cl |
| RE - SC.m | 0.0003 | - | - | - | - | - | - | - |
| LD - SC.m | 0.0269 | 0.10155 | - | - | - | - | - | - |
| PF/MPT - SC.cm | 0.01038 | 0.06615 | 0.05382 | - | - | - | - | - |
| RE - SC.cm | 0.00037 | 0.01038 | 0.02569 | 0.67932 | - | - | - | - |
| LD - SC.cm | 0.03429 | 0.02823 | 0.06615 | 0.14814 | 0.47941 | - | - | - |
| PF/MPT - SC.cl | 0.00514 | 0.8358 | 0.14988 | 0.27131 | 0.12966 | 0.10489 | - | - |
| RE - SC.cl | 0.03429 | 0.06615 | 0.06615 | 0.67771 | 0.8358 | 0.47941 | 0.17882 | - |
| PF/MPT - SC.I | 0.01546 | 0.92727 | 0.44167 | 0.54313 | 0.17882 | 0.17241 | 0.9185 | 0.48076 |
| Branch Path Length | | | | | | | | |
| | PF/MPT - SC.m | RE - SC.m | LD - SC.m | PF/MPT - SC.cm | RE - SC.cm | LD - SC.cm | PF/MPT - SC.cl | RE - SC.cl |
| RE - SC.m | 0.00000072 | - | - | - | - | - | - | - |
| LD - SC.m | 0.01028 | 0.23028 | - | - | - | - | - | - |
| PF/MPT - SC.cm | 0.11847 | 0.00061 | 0.04699 | - | - | - | - | - |
| RE - SC.cm | 0.00000072 | 0.28913 | 0.33678 | 0.00072 | - | - | - | - |
| LD - SC.cm | 0.01654 | 0.03506 | 0.18701 | 0.18701 | 0.06164 | - | - | - |
| PF/MPT - SC.cl | 0.01654 | 0.00148 | 0.04699 | 0.30984 | 0.00548 | 0.77508 | - | - |
| RE - SC.cl | 0.02877 | 0.51997 | 0.18701 | 0.33678 | 0.82103 | 0.77143 | 0.49678 | - |
| PF/MPT - SC.I | 0.03796 | 0.04699 | 0.18701 | 0.26623 | 0.13664 | 0.90476 | 0.82103 | 0.49678 |
| Fractal Dimension | | | | | | | | |
| | PF/MPT - SC.m | RE - SC.m | LD - SC.m | PF/MPT - SC.cm | RE - SC.cm | LD - SC.cm | PF/MPT - SC.cl | RE - SC.cl |
| RE - SC.m | 0.00531 | - | - | - | - | - | - | - |
| LD - SC.m | 0.06165 | 0.88571 | - | - | - | - | - | - |
| PF/MPT - SC.cm | 0.83907 | 0.01258 | 0.08571 | - | - | - | - | - |
| RE - SC.cm | 0.12321 | 0.0526 | 0.18775 | 0.15982 | - | - | - | - |
| LD - SC.cm | 0.18153 | 0.40418 | 0.42562 | 0.35604 | 0.76544 | - | - | - |
| PF/MPT - SC.cl | 0.08397 | 0.00012 | 0.02877 | 0.18775 | 0.00088 | 0.04476 | - | - |
| RE - SC.cl | 0.11424 | 0.42562 | 0.76544 | 0.18701 | 0.63901 | 0.88571 | 0.04476 | - |
| PF/MPT - SC.I | 0.14259 | 0.01258 | 0.04762 | 0.35532 | 0.01258 | 0.04762 | 0.43636 | 0.04762 |
| Fragmentation | | | | | | | | |
| | PF/MPT - SC.m | RE - SC.m | LD - SC.m | PF/MPT - SC.cm | RE - SC.cm | LD - SC.cm | PF/MPT - SC.cl | RE - SC.cl |
| RE - SC.m | 0.00000026 | - | - | - | - | - | - | - |
| LD - SC.m | 0.00621 | 0.06137 | - | - | - | - | - | - |
| PF/MPT - SC.cm | 0.8645 | 0.000025 | 0.01805 | - | - | - | - | - |
| RE - SC.cm | 0.00000026 | 0.00621 | 0.00629 | 0.000013 | - | - | - | - |
| LD - SC.cm | 0.00621 | 0.51997 | 0.15238 | 0.01805 | 0.1981 | - | - | - |
| PF/MPT - SC.cl | 0.0626 | 0.0000064 | 0.00629 | 0.02752 | 0.00000026 | 0.00629 | - | - |
| RE - SC.cl | 0.00621 | 0.64756 | 0.15238 | 0.01805 | 0.31541 | 0.93782 | 0.00629 | - |
| PF/MPT - SC.I | 0.95305 | 0.0001 | 0.02597 | 0.95305 | 0.00018 | 0.02597 | 0.29763 | 0.02597 |
| Height | | | | | | | | |
| | PF/MPT - SC.m | RE - SC.m | LD - SC.m | PF/MPT - SC.cm | RE - SC.cm | LD - SC.cm | PF/MPT - SC.cl | RE - SC.cl |
| RE - SC.m | 0.00000026 | - | - | - | - | - | - | - |
| LD - SC.m | 0.0048 | 0.00057 | - | - | - | - | - | - |
| PF/MPT - SC.cm | 0.00327 | 0.00057 | 0.02017 | - | - | - | - | - |
| RE - SC.cm | 0.0000001 | 2.7E-12 | 0.00046 | 0.0265 | - | - | - | - |
| LD - SC.cm | 0.0048 | 0.03979 | 0.04472 | 0.05331 | 0.06077 | - | - | - |
| PF/MPT - SC.cl | 0.00019 | 0.00103 | 0.00629 | 0.30614 | 0.12993 | 0.12993 | - | - |
| RE - SC.cl | 0.0048 | 0.00057 | 0.04472 | 0.5042 | 0.0048 | 0.04472 | 0.51788 | - |
| PF/MPT - SC.I | 0.0024 | 0.05331 | 0.04762 | 0.06679 | 0.33766 | 0.55556 | 0.12993 | 0.03008 |
| Number of Branches | | | | | | | | |
| | PF/MPT - SC.m | RE - SC.m | LD - SC.m | PF/MPT - SC.cm | RE - SC.cm | LD - SC.cm | PF/MPT - SC.cl | RE - SC.cl |
| RE - SC.m | 0.00022 | - | - | - | - | - | - | - |
| LD - SC.m | 0.01835 | 0.10961 | - | - | - | - | - | - |
| PF/MPT - SC.cm | 0.00951 | 0.05037 | 0.05037 | - | - | - | - | - |
| RE - SC.cm | 0.00022 | 0.00951 | 0.01835 | 0.66578 | - | - | - | - |
| LD - SC.cm | 0.01835 | 0.01835 | 0.06367 | 0.26852 | 0.64114 | - | - | - |
| PF/MPT - SC.cl | 0.00323 | 0.74031 | 0.12302 | 0.18623 | 0.12793 | 0.06367 | - | - |
| RE - SC.cl | 0.01835 | 0.05037 | 0.06367 | 1 | 0.95915 | 0.4047 | 0.10961 | - |
| PF/MPT - SC.I | 0.0156 | 1 | 0.48076 | 0.23764 | 0.10961 | 0.95915 | 0.41544 | - |
| Height/Width Ratio | | | | | | | | |
| | PF/MPT - SC.m | RE - SC.m | LD - SC.m | PF/MPT - SC.cm | RE - SC.cm | LD - SC.cm | PF/MPT - SC.cl | RE - SC.cl |
| RE - SC.m | 0.00000059 | - | - | - | - | - | - | - |
| LD - SC.m | 0.00527 | 0.04482 | - | - | - | - | - | - |
| PF/MPT - SC.cm | 0.00527 | 0.00016 | 0.01797 | - | - | - | - | - |
| RE - SC.cm | 0.0000021 | 0.00527 | 0.0058 | 0.00246 | - | - | - | - |
| LD - SC.cm | 0.00527 | 0.00527 | 0.04114 | 0.12857 | 0.04482 | - | - | - |
| PF/MPT - SC.cl | 0.00016 | 0.01797 | 0.01185 | 0.01518 | 0.94875 | 0.09375 | - | - |
| RE - SC.cl | 0.00527 | 0.09805 | 0.04114 | 0.02981 | 0.93215 | 0.12857 | 0.84875 | - |
| PF/MPT - SC.I | 0.00343 | 0.07907 | 0.79654 | 0.00974 | 0.00016 | 0.02597 | 0.0045 | 0.02597 |